Calculating the Band Structure of Photonic Crystals through the Meshless Local Petrov-Galerkin (MLPG) Method and Periodic Shape Functions

Williams L. Nicomedes[1], Renato C. Mesquita[2], and Fernando J. S. Moreira[1]
Depts. of [1]Electronic and [2]Electrical Engineering, Federal University of Minas Gerais
Av. Antonio Carlos 6627, 31270-901, Belo Horizonte, Brazil
wlnicomedes@yahoo.com.br, renato@ufmg.br, fernandomoreira@ufmg.br

***Abstract* — This paper illustrates how to determine the bandgap structure of photonic crystals through meshless methods. These methods are generally akin to the Finite Element Method (FEM), as they also deal with the discretization of weak forms and produce sparse stiffness matrices. The major difference is the complete absence of whatever kind of mesh. We concentrate in a particular method, the Meshless Local Petrov Galerkin 4 (MLPG4), also known as Local Boundary Integral Equation Method (LBIE). Since the boundary conditions governing the electromagnetic fields are periodic in a unit cell, we develop a special scheme to embed this feature on the shape functions used to approximate the field. As a result, the boundary conditions do not need to be imposed on the unit cell.**

I. INTRODUCTION

The seminal idea underlying all meshless methods is to be able to build numerical solutions to differential equations defined in a certain geometrical domain *without* resorting to a mesh or a grid set up in this domain. The first studies concerning the use of meshfree techniques were reported in the early past decade, in the field of Computational Mechanics [1]. In Electromagnetics there have been such appearances like [2], where a method called Element-Free Galerkin (EFG) has been employed. EFG is not truly regarded as a meshless method, because background cells are necessary to perform the numerical integrations [1]. In MLPG, the integrations are carried out within certain local domains, what dismisses the use of whatever kind of background cells [3].

The MLPG method employs two kinds of functions, *shape* and *test functions*, which belong to two different spaces. The shape functions are constructed numerically, whilst there are many choices available to the test functions. We are particularly interested in MLPG4/LBIE, whose test function is a solution to Green's problem for Laplace's equation. The MLPG4/LBIE method was successfully applied to situations in 2D electromagnetic wave scattering [5] and in 3D Electrostatics [6]. We now move on and look for applications of MLPG4 to eigenvalue problems, specifically those arising in the analysis of 2D photonic bandgap crystals. After a sketch on the general idea behind meshless methods and some discussion on periodic shape functions, we present an example concerning the band structure of a photonic crystal for incoming TM^z waves.

II. MESHLESS METHODS: OVERVIEW AND SHAPE FUNCTIONS

Let Ω be a two-dimensional domain (global boundary $\partial\Omega$). In order to find a numerical approximation u^h for a function u, we begin by spreading nodes across the domain. The nodal distribution need not be uniform (even random distributions can be used). The next step is to define shape functions associated to each node. These functions do not have analytical expressions, and therefore require a numerical scheme to be constructed. Usually, a shape function associated to a node depends on the relative positions of neighboring nodes. Furthermore, shape functions are compactly supported, i.e., they are different from zero only at a small region surrounding the node (called the node's *influence domain*). It is this very property which renders the final stiffness matrix sparse. So, given a point $\vec{x}$ where u^h shall be calculated there follows:

$$u(\vec{x}) \cong u^h(\vec{x}) = \sum_i \phi_i(\vec{x})\hat{u}_i = \boldsymbol{\Phi}(\vec{x})\hat{\boldsymbol{u}} \qquad (1)$$

where the global index i runs through all nodes whose influence domains include point $\vec{x}$ and each $\hat{u}_i$ is a coefficient that shall be determined (also called *nodal parameter*). A constraint must be satisfied: the union of the influence domains from all nodes must cover the whole domain. The size of the influence domains can be adjusted, but should not be set too large. Overlapping of influence domains is freely allowed.

There are many ways in which the shape functions can be constructed. In this work, a procedure called Moving Least Squares (MLS) has been employed [1]. In order to get the MLS shape functions, one usually has to go through a rather extensive numerical calculation involving matrices. Given a point $\vec{x}$ at which the shape functions are to be calculated, one first finds all neighboring nodes which extend their influence domains until $\vec{x}$ (for example, nodes with global indices 3, 5, 10 and 18, say, act upon $\vec{x}$). Then one feeds all this information in a numerical procedure and finally gets the shape functions calculated at $\vec{x}$:

$$\boldsymbol{\Phi}(\vec{x}) = [\phi_3(\vec{x}), \phi_5(\vec{x}), \phi_{10}(\vec{x}), \phi_{18}(\vec{x})] = \boldsymbol{p}^T\boldsymbol{A}^{-1}\boldsymbol{B} \qquad (2)$$

where $\boldsymbol{p}$, $\boldsymbol{A}$ and $\boldsymbol{B}$ are matrices which depend on $\vec{x}$ and on the coordinates of the neighbor nodes [4]-[5].

III. CALCULATING THE BAND STRUCTURE OF A PHOTONIC CRYSTAL: THE LBIE METHOD

In LBIE, to each node i at $\vec{x}_i$ is ascribed a test function v_i, in addition to a shape function ϕ_i. This test function acts in a specific region Υ_i surrounding the node, called *test domain*. In LBIE, the test domain is required to be a *circle* centered at each node, and must satisfy: $\nabla^2 v_i(\vec{x}) = -\delta(\vec{x} - \vec{x}_i)$ (a Dirac delta at $\vec{x}_i$) and $v_i(\vec{x}) = 0$ at the test domain boundary $\partial\Upsilon_i$. A function v_i satisfying the above requirements is given by $v_i(\vec{x}) = (1/2\pi)\ln(s_i/\|\vec{x} - \vec{x}_i\|)$. In this work, the radii of all test (s_i) and influence (r_i) domains are equal.

A two-dimensional photonic bandgap crystal is a periodic array of dielectric structures, the most remarkable

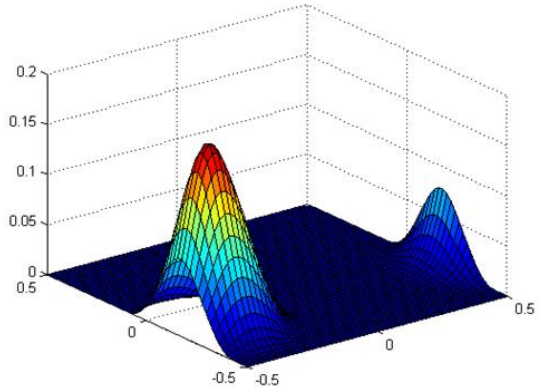

Fig. 1. A periodic MLS shape function in the domain $\Omega = [-0.5,0.5] \times [-0.5,0.5]$. It can be verified that this shape function ϕ satisfies boundary conditions (4). The periodicity of the function u has been embedded in the shape functions used to approximate it.

property of which is that it is able to select what wavelengths can actually propagate through it. A unit cell is a pattern that is replicated throughout the space in order to generate the crystal. The mathematical analysis is usually confined to a single cell, which coincides with our computational domain Ω. For an incoming TM^z wave (electric field pointing at $\hat{\boldsymbol{z}}$), the problem is modeled by the Helmholtz equation for the electric field E_z and Bloch-periodic boundary conditions [6]. However, according to Bloch's theorem, the electric field E_z can be written as $E_z(\vec{x}) = e^{-j\vec{K}.\vec{x}}u(\vec{x})$, where u is now a periodic function in Ω and $\vec{K}$ is the Bloch vector. Substituting this new form for E_z, we get an equivalent problem:

$$-\nabla^2 u + j2\vec{K}\cdot\nabla u + \left\|\vec{K}\right\|^2 u = (\omega/c)^2\varepsilon_r u \qquad (3)$$

$$u(\vec{x}+\vec{L}) = u(\vec{x}) \text{ and } \partial u(\vec{x}+\vec{L})/\partial n = \partial u(\vec{x})/\partial n \qquad (4)$$

Boundary conditions (4) tell us that the function u (and its normal derivative) at one side of $\partial\Omega$ is equal to u at the opposite side ($\vec{L}$ is the lattice translation vector). So u is periodic in a unit cell Ω. In order to solve (4), nothing seems more natural than to find shape functions which are also periodic in Ω. We found a very simple way to construct these shape functions. It boils down to considering an extra layer of cells around Ω and to applying (2) to this new extended domain. If our computational domain Ω happens to be $\Omega = [-0.5,0.5] \times [-0.5,0.5]$, Fig. 1 shows how a periodic MLS shape function associated to a given node would look like. If all shape functions satisfy (4), then a linear combination of ϕ's also will, i.e., the ϕ's form a vector space of functions periodic in Ω. Therefore, boundary conditions (4) no longer need to be imposed. In order to find the weak form for (3), we take each node i and apply Green's second identity to u and v_i, getting a local integral equation:

$$u(\vec{x}_i) + \oint_{\partial\Upsilon_i} u\frac{\partial v_i}{\partial n}dl + \iint_{\Upsilon_i}\left(j2\vec{K}\cdot\nabla u + \left\|\vec{K}\right\|^2 u\right)v_i\,dS = \left(\frac{\omega}{c}\right)^2\iint_{\Upsilon_i}\varepsilon_r u v_i dS \qquad (5)$$

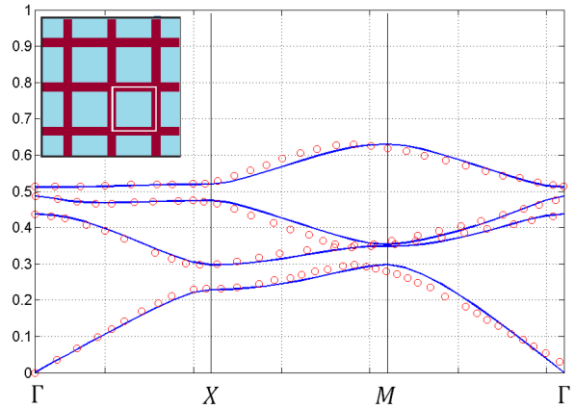

Fig. 2. Band structure for the crystal formed by dielectric veins. Blue lines: MLPG4, Red balls: reference [7]. At the inset, the light blue regions are characterized by $\varepsilon_r = 1$, whereas the grating (veins) has $\varepsilon_r = 8.9$. The region inside the white square is the unit cell Ω.

Instead of Green's identity, one can also apply the weighted residual method, and thus get a slightly different weak form, in which the first two terms of (5) are substituted by an area integral involving $\nabla u \cdot \nabla v_i$. The final step is to enforce (5) at all nodes in Ω, and calling upon (1) whenever u appears. As a result, we get a generalized eigenvector problem of the type $\boldsymbol{R}\hat{\boldsymbol{u}} = \beta\boldsymbol{T}\hat{\boldsymbol{u}}$, which is readily solved for the eigenvalues $\beta = (\omega/c)^2$. $\boldsymbol{R}$ and $\boldsymbol{T}$ are sparse matrices.

Figure 2 illustrates the band structure concerning the four first eigenvalues (normalized to $\omega a/2\pi c$), for the Bloch vector varying from point $\boldsymbol{\Gamma}$ ($\vec{K} = [0,0]$) to point $\boldsymbol{X}$ ($\vec{K} = [\pi/a\,, 0]$), from $\boldsymbol{X}$ to $\boldsymbol{M}$ ($\vec{K} = [\pi/a\,, \pi/a]$), and finally from $\boldsymbol{M}$ back to $\boldsymbol{\Gamma}$. The crystal is a square array of dielectric veins ($\varepsilon_r = 8.9$ and thickness $0.165a$, at the inset). The domain Ω is a square whose side is a (normalized to 1, as in Fig. 1), and the results are compared to those shown in [7]. Even though only approximately 200 nodes have been scattered throughout Ω, and despite a coarse numerical integration employed in (5), a good agreement has been obtained.

IV. REFERENCES

[1] G. R. Liu, *Mesh Free Methods: Moving Beyond the Finite Element Method*. CRC Press, 2003.

[2] A. Manzin, and O. Bottauscio, "Element-free Galerkin method for the analysis of electromagnetic-wave scattering", *IEEE Trans. Magnetics*, vol. 44, no 6, pp. 1366-1369, 2008.

[3] S. Atluri and S. Shen, "The Meshless Local Petrov-Galerkin Method: A simple & less-costly alternative to the finite-element and boundary element methods", *CMES*, vol. 3, no 1, pp 11-51, 2002.

[4] W. Nicomedes, R. Mesquita, and F. Moreira, "A Local Boundary Integral Equation (LBIE) Method in 2D Electromagnetic Wave Scattering, and a Meshless Discretization Approach", *Proc. of the SBMO/IEEE MTT-S Int. Microw.Optoelec. Conf.*, pp. 133-137, 2009.

[5] W. Nicomedes, R. Mesquita, and F. Moreira, "A Meshless Local Boundary Integral Equation Method for Three Dimensional Scalar Problems", *IEEE Transactions on Magnetics*, to be published.

[6] I. Tsukerman, *Computational Methods for Nanoscale Applications*, Nanostructure Science and Technology Series, Springer, 2008.

[7] J. D. Joannopoulos, S.G. Johnson, J. N. Winn and R. D. Meade, *Photonic Crystals: Molding the Flow of Light*, Princeton University Press,2008,p.72.